

Rare earth element geochemistry of hydrothermal deposits from Southwest Indian Ridge

CAO Zhimin¹, CAO Hong^{1,2*}, TAO Chunhui³, LI Jun², YU Zenghui¹, SHU Liping^{1,4}

¹ Key Laboratory of Submarine Geosciences and Technology, Ministry of Education, Department of Marine Geoscience, Ocean University of China, Qingdao 266100, China

² Key Laboratory of Marine Hydrocarbon Resources and Environment Geology MLR, Qingdao Institute of Marine Geology, Qingdao 266071, China

³ Laboratory of Submarine GeoScience, Second Institute Oceanography, State Oceanic Administration, Hangzhou 310012, China

⁴ Petrology of the Oceanic Crust, Geosciences Department, University of Bremen, Bremen 28359, Germany

Received 6 May 2011; accepted 20 October 2011

© The Chinese Society of Oceanography and Springer-Verlag Berlin Heidelberg 2012

Abstract

The REE compositions of hydrothermal deposits and basalt samples from the Southwest Indian Ridge (SWIR) were determined with ICP-MS. The results show that there are significant differences between different types of samples although all samples show relative LREE enrichment. The contents of REE in hydrothermal sulfides and altered rocks samples are lower (from 7.036×10^{-6} to 23.660×10^{-6}), while those in the white chimney deposits are relatively higher (ranging from 84.496×10^{-6} to 103.511×10^{-6}). Both of them are lower than basalts. Chondrite-normalized REE distribution patterns show that sulfides and altered rocks samples are characterized by significant positive Eu anomalies. On the contrary, white chimney deposits have obvious negative Eu anomalies, which may be caused by abundant calcite existing in the white chimney samples. Both the content and distribution pattern of REE in sulfides suggest that REE most possibly is originally derived from hydrothermal fluids, but influenced by the submarine reducing ore-forming environment, seawater convection, mineral compositions as well as the constraint of mineral crystallizations.

Key words: rare earth element, hydrothermal deposits, Southwest Indian Ridge

1 Introduction

After the discovery of high-temperature black smokers on the East Pacific Rise (EPR) 21°N (Equipe, 1979), the study of sea-floor hydrothermal mineralization has largely been focused on the rapid spreading ridge of the East Pacific. It was once believed that such high-temperature vents only occurred on the rapid to intermediate spreading ridges until the high-temperature hydrothermal sulfide deposits were found at the slow spreading Mid-Atlantic Ridge (Rona et al., 1986; Li et al., 2008). Due to its low thermal budget, SWIR was once considered impossible to develop high-temperature hydrothermal activities. In order to search this ridge for hydrothermal vent sites and sulfide deposits, submersible investigations focus on the fissures and chasms, which may strengthen fluids convection. During the Indoyo cruise with Japan

Yokosuka investigation ship in 1998, relict hydrothermal sulfides, hydrothermal chimneys and hydrothermal mounds were found in the east of the Melville fracture zone (27°51'S, 63°56'E), whose ages were determined varying between 70 000 and 13 000 years (Münch et al., 2001). This discovery proves that high-temperature sulfide chimneys can also develop at ultra-slow spreading ridge such as the Southwest Indian Ridge. Furthermore, the sulfide samples from this field show great differences in their mineralogical, as well as chemical compositions, when compared with sulfide samples from rapid spreading ridge environment (Münch et al., 2001). So, this discovery provides a new chance to better understanding the global mid-ocean ridge hydrothermal system, thus greatly enriching the hydrothermal mineralization theory.

The special tectonic environment of ultra-slow spreading segment on Southwest Indian Ocean Ridge

Foundation item: The National Natural Science Foundation of China under contract No. 40872063.

*Corresponding author, E-mail: caohong_qingdao@126.com

provides us an excellent natural laboratory, and meanwhile it is a major break point for further understanding of the earth about the internal dynamics state, deep structure, origin and evolution of magma. In the slow-spreading ridges, the low frequency of tectonic events may avail to sustain long life hydrothermal upwelling and multi-period events, and much more conducive to the formation of large deposits, compared with highly unstable hydrothermal systems on the fast spreading ridges (Charlou et al., 1998; Li, 2007).

Because of the unique geochemical characteristics, the rare earth elements play a major role in inferring chemical evolution and material sources of hydrothermal fluid. The REE geochemical characteristics of hydrothermal chimneys and hosted basalt obtained from the Southwest Indian Ocean ridge were firstly determined and the material sources and evolution mechanism of the REE were discussed also in this paper.

2 Samples

Two recent Global Ocean Expeditions organized by China Ocean Association in 2007 and 2008, have successfully discovered the first active hydrothermal vent field at the Southwest Indian Ridge and also recovered hydrothermal sulfide deposit samples in the vent sites (Tao et al., 2007). In the second cruise, a large range of 20 km² of new type calcium carbonate "white chimney" hydrothermal field has also been detected (Song, 2009).

The samples recovered during the Global Ocean Expedition are shown in Table 1 and Fig. 1. Sample AIR 1 and AIR 2 are sulfides recovered during the first cruise. Sample ISU 1, ISU 2, ISU 4, ISU 5, IBA 1 and IBA 2 were recovered during the second cruise, in which ISU 1 and ISU 2 are sulfides, ISU 4 and ISU 5 white chimney deposits, IBA 1 and IBA 2 basalts.

Table 1. Sampling stations

Sample No.	Station		Water depth /m
	East longitude(°)	South latitude(°)	
AIR1	69.596 7	23.878 0	3 292
AIR2	69.596 7	23.878 0	3 292
ISU1	49.648 1	37.780 2	2 783
ISU2	50.467 2	37.658 6	1 740
ISU4	50.945 5	37.624 0	2 098
ISU5	51.009 1	37.600 0	2 034
IBA1	50.473 1	37.658 2	1 751
IBA2	49.647 8	37.783 9	2 825

The mineral composition identification and analysis using the electronic microscope and X ray diffrac-

tion (Fig. 2) method, are as follows:

AIR 1 is yellow and porous sulfide, with a clear mineral zoning. AIR 1 is possibly collapsed sulfide chimney, mainly consisting of sphalerite and pyrite, in addition to chalcopyrite, sphalerite, small amounts of barite and quartz. Sample AIR 2 is also collapsed sulfide chimney, with a red out layer and black inner core, mainly consisting of pyrite, marcasite and gypsum, a small amounts of quartz, chalcopyrite and sphalerite. The ISU 1 in dark color and with massive structure and oxides crust, is mainly composed of lepidocrocite and chalcopyrite, a small amount of pyrite, marcasite, sphalerite, gypsum, barite and quartz. The yellow and porous ISU 2 with obvious mineral zoning has the outermost crust composed of loose black material and a color change to the inner from brown zone to reddish yellow zone. The most inner layer is pale yellow zone with poor crystallinity, and mainly consists of kurnakovite, lizardite, manganese oxide and iron alum mineral, inferred to be hydrothermal altered ultramafic rocks. Sample ISU 4 and ISU 5 are wheat and white loose crumby respectively. Most minerals are calcite, and a small amount of magnesium calcite and zeolite. Sample IBA 1 and IBA 2 are pillow basalts with 5 mm thick fresh glassy rim covered by weathered brown-black film. Rock-forming minerals mainly are plagioclase and pyroxene.

3 Test method of the samples

Major elements (Ca and Mg) and REE were respectively analyzed by Inductively Coupled Plasma-Atomic Emission Spectrometry (ICP-AES) and Inductively Coupled Plasma-Mass Spectrometry (ICP-MS), which has high sensitivity and low detection limit. First, the samples were vibrated and cleaned using ultrapure water. They were subsequently dried at low temperature and grinded into powder (less than 200 meshes in size) within an agate mortar. Then, the samples were dried at 105 °C for 3 h in an oven. Finally, they were cooled for 24 h in dryer.

The samples of 0.04 g weighed using high precision balance of ten thousandth of the scale were putted into digestion tank and digested in approximately 2 ml mixed acid (HNO₃:HF=10:1). They were subsequently shaken gently, then microwave digestion program was executed. The solutions were transferred

into PTFE crucible, and heated to nearly dry on electric heating plate. When heating until the white smoke disappeared, 2 ml of 2% HNO_3 was added. These crucibles were removed, cooling. The solutions were transferred to vials, rinsing crucible wall three times using ultrapure water, and then diluted to 20 g with 2% HNO_3 (A). After shaking, 5 g sample solution was

picked up with pipette gun, and diluted to 20 g with 2% HNO_3 again. They were shaking again (B), at last, the solution A and solution B were respectively analyzed by ICP-AES (OPTIMA4300, Perkin Elmer) and ICP-MS (Agilent 7500c, Agilent Technologies) at “element and isotope analysis laboratories” of Marine Geosciences, Ocean University of China.



Fig.1. Pictures of sample.

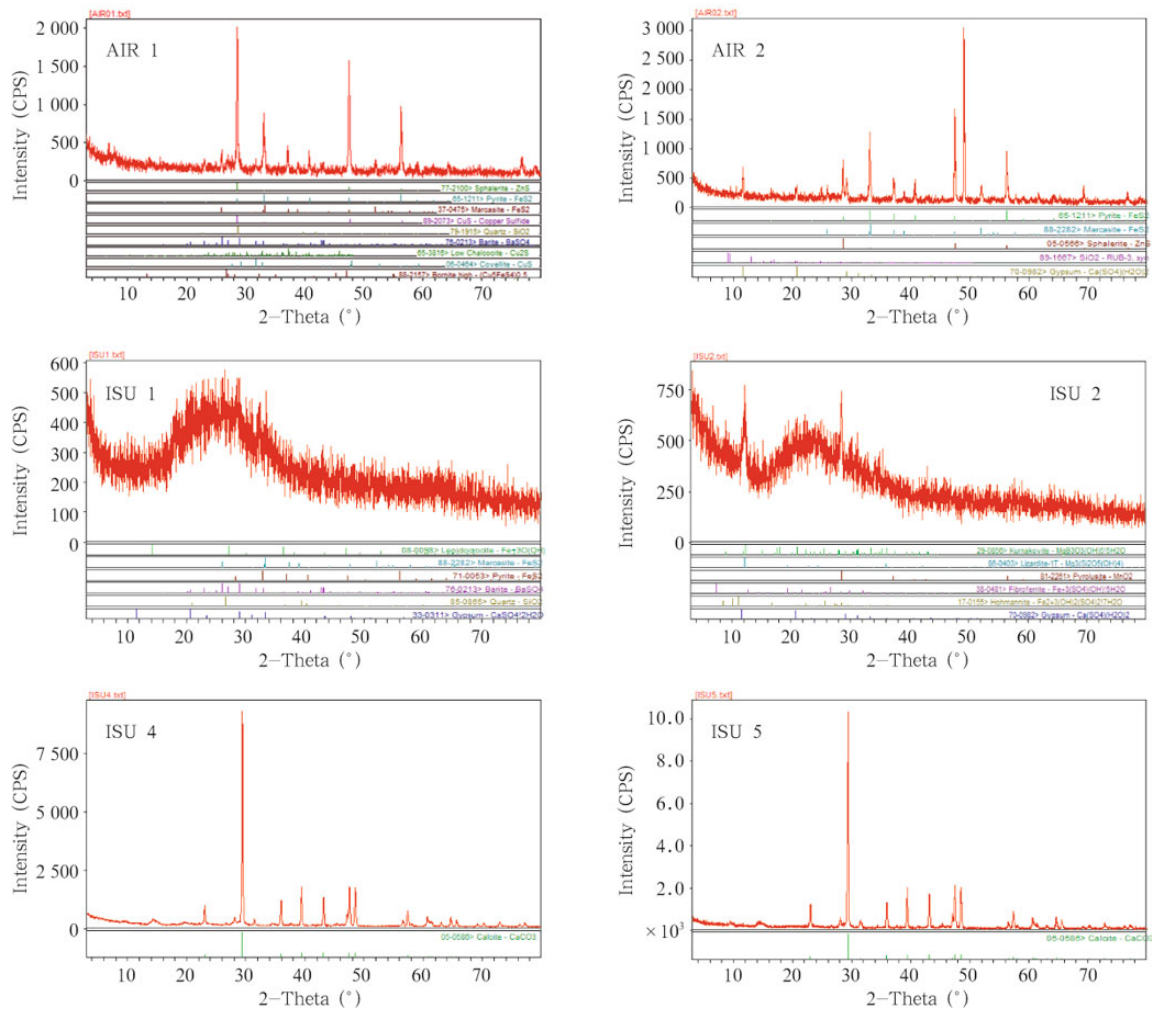


Fig. 2. X diffraction figure of samples.

In order to ensure the reliability of data the parallel samples were added to each samples, and blank and standard material (GBW07312) added together in this study. The analysis value of standard material was consistent with the given value, and repeatability was less than 10%.

4 Results

The REE contents analysis results and characteristic parameters are shown in Table 2, and the chondrite standard data of REE are quoted from Boynton (1984).

As shown in Table 2, different types of hydrothermal deposits samples have large difference in REE contents. The REE contents of hydrothermal altered rocks are lower (7.036×10^{-6}). REE content of hydrothermal sulfides have a range from 17.117×10^{-6} to 23.660×10^{-6} lower than those of the white chim-

ney deposit of which the REE content varies from 84.496×10^{-6} to 103.511×10^{-6} .

The REE Chondrite-normalized distribution patterns of samples are shown in Fig. 3 from which both differences and similarities between the black hydrothermal chimneys and white chimneys can be found. Hydrothermal altered rocks and sulfides samples are characterized by significant positive Eu anomalies ($\delta\text{Eu}=1.252\text{--}11.520$) and the enrichment of LREE relative to HREE. Meanwhile, they also have slightly negative Ce anomalies ($\delta\text{Ce}=0.722\text{--}0.811$). It is impossible for deposits to show negative Ce anomalies just by precipitation from conduction-cooled hydrothermal fluid, and only when the convection mixing happened, deposition can bear both Eu positive anomalies and negative Ce anomalies (Ding et al., 2000). Therefore, negative Ce anomalies, superposing on the significant positive Eu anomalies, may indicate the convection mixing between hydrothermal fluid and

seawater before the precipitation of the sulfides. While the white chimney samples manifest obvious negative Eu and Ce anomalies, varying in a small range ($\delta\text{Eu}=0.578\text{--}0.615$, $\delta\text{Ce}=0.454\text{--}0.471$). The slope of Chondrite-normalized distribution curve of hydrothermal black and white chimneys are similar to each other. $(\text{La}/\text{Yb})_{\text{N}}$ values change in the range of 2.899–

19.027, showing the relative enrichment of LREE to HREE (Fig. 3). Different samples also show different degree fractionation between LREE or HREE. $(\text{La}/\text{Sm})_{\text{N}}$ changes from 2.460 to 8.152, indicating that the LREE has a clear fractionation; and $(\text{Gd}/\text{Yb})_{\text{N}}$ range from 1.004 to 2.196, indicating that the HREE fractionation is weak.

Table 2. REE contents (10^{-6}) and parameters of hydrothermal deposition from SWIR

Element	AIR1	AIR2	ISU1	ISU2	ISU4	ISU5	IBA1	IBA2
La	6.227	4.397	4.62	1.20	27.75	24.11	9.19	12.95
Ce	8.982	7.238	7.452	1.931	26.700	22.280	26.570	33.150
Pr	0.855	0.747	0.691	0.272	5.118	4.274	4.739	5.274
Nd	3.242	3.017	2.578	1.400	22.640	18.590	27.200	28.530
Sm	0.566	0.543	0.357	0.306	4.503	3.493	8.775	8.317
Eu	2.141	1.448	0.147	0.369	0.889	0.652	2.195	2.200
Gd	0.510	0.424	0.326	0.347	3.764	2.962	8.598	7.722
Tb	0.076	0.063	0.046	0.052	0.697	0.458	2.134	1.785
Dy	0.399	0.362	0.294	0.425	4.327	2.990	12.070	10.150
Ho	0.062	0.050	0.051	0.083	0.885	0.587	2.453	2.022
Er	0.272	0.231	0.281	0.279	2.717	1.808	7.254	6.010
Tm	0.038	0.028	0.029	0.046	0.401	0.272	1.113	0.902
Yb	0.247	0.156	0.209	0.278	2.703	1.740	7.399	5.996
Lu	0.044	0.028	0.032	0.051	0.417	0.281	1.081	0.882
Y	1.851	1.331	1.525	2.531	3.427	76.540	27.850	56.860
LREE/HREE	13.360	12.952	12.497	3.506	5.506	6.614	1.869	2.549
$\sum\text{REE}$	23.660	18.733	17.117	7.036	103.511	84.496	120.771	125.890
δEu	11.520	8.463	1.252	3.394	0.615	0.578	0.741	0.798
δCe	0.722	0.811	0.802	0.775	0.471	0.454	1.229	1.137
$(\text{La}/\text{Yb})_{\text{N}}$	17.017	19.027	14.895	2.899	6.922	9.342	0.837	1.456
$(\text{La}/\text{Sm})_{\text{N}}$	6.925	5.090	8.152	2.460	3.876	4.342	0.659	0.979
$(\text{Gd}/\text{Yb})_{\text{N}}$	1.668	2.196	1.255	1.004	1.124	1.374	0.938	1.039
Ba	1 396	1 537	100.5	316.8	121	133.6	74.73	129.6
Ca(%)	0.746	1.511	0.794	0.287	28.579	32.914	7.052	7.357

5 Discussion

(1) Material source

REE chondrite-normalized distribution patterns of hydrothermally altered rocks and sulfides samples are different from underlying basalts, also quite different from seawater (Fig. 3). However, they are rather similar to the high-temperature hydrothermal fluids occurring on global ridges with different tectonic settings and base rock type (Klinkhammer, 1994). Hydrothermal fluids investigation (Michard et al., 1983; Michard and Alharedo, 1986; Michard, 1989) indicates that submarine high-temperature hydrothermal fluids generally show LREE (La-Gd) enrichment and significant positive Eu anomalies (Ding et al., 2000). Therefore, the REE in hydrothermal sulfides from the SWIR hydrothermal fields maybe mainly derive from hydrothermal fluids.

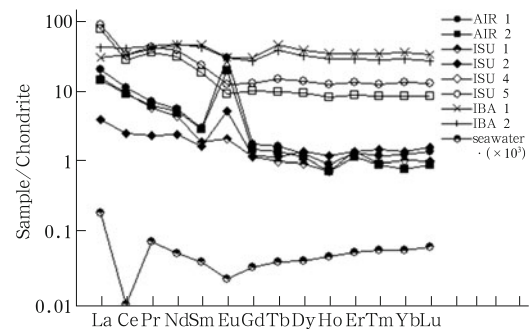


Fig. 3. Chondrite-normalized REE patterns of hydrothermal deposits and basalts samples from SWIR. The REE content data of seawater quoted from (Gillis et al., 1990).

(2) Precipitation mechanism of REE

Different types of hydrothermal sedimentary samples of SWIR have different REE contents and distribution pattern. The REE contents of hydrothermally altered rocks are lower. REE contents of hy-

drothermal sulfides are lower than those of the white chimney deposits. The concentrating of REE in calcite ore (Michard, 1989) may be the reason for the relatively high content (84.50×10^{-6} – 103.51×10^{-6}) of REE in the white chimney deposits which are mainly composed of calcite. REE contents of these samples show a good positive correlation relationship with Ca (Fig. 4).

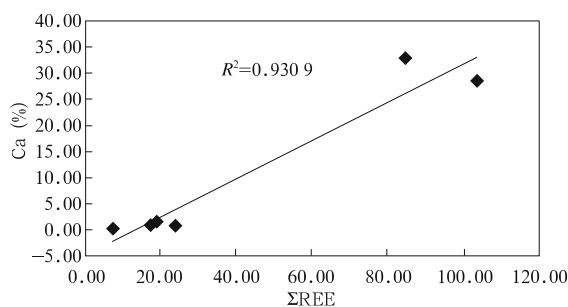


Fig.4. The correlation of Σ REE and Ca of hydrothermal deposits from SWIR.

The chondrite-normalized pattern of white chimney deposit is right-lean type, namely, the relative enrichment of light rare earth elements (LREE). As ionic radius of LREE^{3+} is more similar to that of Ca^{2+} than HREE^{3+} , the LREE is easier to replace the lattice of Ca^{2+} than HREE^{3+} when REE come into hydrothermal calcites mainly by the replacement of REE^{3+} for Ca^{2+} . In addition, as REE mainly exists as complex in solution, the complex stability of REE to CO_3^{2-} and HCO_3^- increases with the increase of atomic number of REE (Wood, 1990; Lottermoser, 1992; Haas et al., 1995; Terakado and Masuda, 1988; Cantrell et al., 1987; Shuang et al., 2006). Therefore, the REE distribution coefficients between calcite and fluid decreases with the increase of atomic number (Wood, 1990; Zhong and Mueei, 1995; Rimstidt et al., 1998; Shuang et al., 2006). The above two points may codetermine the relative enrichment of LREE of white chimney.

δEu value plays a significant role in the REE geochemistry, and is an important reference for the discussion of mineralization condition. In relatively reducing conditions, the REE contents are generally high in calcite and the chondrite-normalized pattern gives Eu negative anomalies (Liang et al., 2007). This fact suggests that the white chimney deposits formed in a reduced environment. Liu et al. (2005) studied REE elements of massive sulfides from Jade hydrothermal field in the central Okinawa Trough and found that the intensity of Eu anomaly is proportional with

the barium content in both the copper-zinc sulfide ore, recrystalline-amorphous SiO_2 type ore. Considering that when the solution temperature higher than 250°C Eu in the form of Eu^{2+} will have the ion radius roughly similar to Ba^{2+} , and will instead Ba^{2+} into the BaSO_4 mineral with hydrothermal fluid venting out from the sea floor and sulfides rapidly precipitating. The correlation coefficient between δEu and Ba is high up to 0.91 in hydrothermal samples (Fig. 5), which may be another reason for the positive Eu anomalies occurring in sulfides. As there is still lack of the temperature of hydrothermal fluids in the study areas, the above inference remains to be verified.

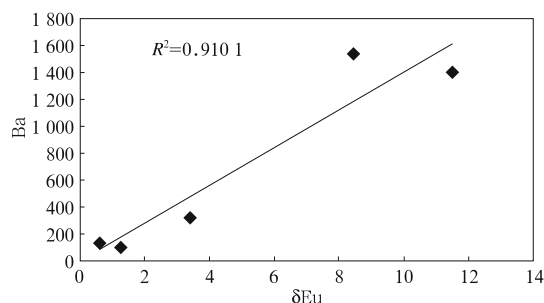


Fig.5. The correlation of δEu and Ba of hydrothermal deposits from SWIR.

(3) Comparison of different ridge

The REE contents of hydrothermal sulfides from SWIR (average of 19.83×10^{-6}) is obviously higher than those of from East Pacific Rise (EPR9-10°N) ($\text{REE} = 0.481 \times 10^{-6}$) (An, 2006) and Atlantic (TAG) ($\text{REE} = 1.595 \times 10^{-6}$) (Zeng et al., 1999). However, the Chondrite-normalized REE distribution patterns are approximately same, namely, characterized by significant positive Eu anomalies and the enrichment of LREE relative to HREE. REE contents of hydrothermal sulfide show a good positive correlation relationship with REE in water solution, while the latter is associated with the rock type occurrence of water rock interaction (Annette and Robert, 1991), thus the REE contents of hydrothermal sulfides from different hydrothermal area reflect the difference of rock mineral components.

6 Conclusions

(1) The REE contents is low in hydrothermally altered rocks and sulfides samples from the South West Indian Rige. Chondrite-normalized REE patterns show significant positive Eu anomalies and LREE enrichment, inheriting the characteristics of hydrother-

mally fluids, and suggesting that the REE in hydrothermal altered rocks and sulfides may be mainly derived from hydrothermal fluids.

(2) The REE contents are high in the white chimney deposits dominantly composed of calcite. Significant negative Eu anomalies may indicate the relative reduction mineralization conditions.

(3) Insteadance of Eu^{2+} for Ba^{2+} into the BaSO_4 lattice may be another reason for Eu anomalies of the hydrothermal samples. However, the inference remains to be verified as there is still lack of the temperature of hydrothermal fluids in the study areas.

(4) Hydrothermal deposits samples from different ridge are different in REE contents. It reflects the difference of rock mineral components during water rock interaction in the hydrothermal activity.

Acknowledgements

The authors appreciate the assistance of China Ocean Samples Repository and Prof. Zhai Shikui in providing valuable samples for this experiments, and also grateful to engineer Zhang Aibin from “element and isotope analysis laboratory”, Marine Geosciences, Ocean University of China, for his valuable advice and selfless help for this experiment.

References

- An Wei. 2006. Characteristics and control factors of modern seafloor hydrothermal ore-forming processes [dissertation]. Qingdao: Ocean University of China Marine Geology Department
- Annette M O, Robert M O. 1991. The europium anomaly of seawater: implication for fluvial versus hydrothermal REE inputs to the Oceans. *Chemical Geology*, 92: 317–328
- Boynnton W V. 1984. Cosmochemistry of the earth elements: Meteorite studies. In: Henderson P, ed. *Rare Earth Element Geochemistry*. Amsterdam: Elsevier, 63–114
- Cantrell K J, Huiday A N, Scrivener R C. 1987. Samarium-Neodymium direct dating of fluorite mineralization. *Science*, 252: 949–951
- Charlou J L, Fouquet Y, Bougauh H, et al. 1998. Intense CH_4 plumes generated by serpentinization of ultramafic rocks at the intersection of the $15^\circ 20' \text{N}$ fracture zone and the Mid-Atlantic ridge. *Geochimica et Cosmochimica Acta*, 62: 2323–2333
- Ding Zhenju, Liu Congqiang, Yao Shuzhen et al. 2000. Rare earth elements compositions of high-temperature hydrothermal fluids in sea floor and control factors. *Advances in Earth Science*, 15(3): 307–312
- Equipe Scientifique Cyamex. 1979. Découverte par submersible de sulfures polymetal liques massifs sur la dorsale du Pacifique oriental, par 21°N (projet RITA). *C R Acad Sci*, 287: 365–368
- Gillis K M, Smith A D, Ludden J N. 1990. Trace element and Sr isotopic contents of hydrothermal clays and sulfides from the Snakepit hydrothermal field: ODP site 649. *Proc ODP Sci Res*, 106/109: 315–319
- Haas J R, Everett L, Shock, et al. 1995. Rare earth elements in hydrothermal systems: Estimates of standard partial molal thermodynamic properties of aqueous complexes of the rare earth elements at high pressures and temperatures. *Geochimica et Cosmochimica Acta*, 59(21): 4329–4350
- Klinkhammer G P, Elderfield H, Mitra A. 1994. Geochemical implications of rare earth element patterns in hydrothermal fluids from mid-ocean Ridges. *Geochim Cosmochim Acta*, 88: 5105–5113
- Li Wenyuan. 2007. Classification, distribution and forming setting of massive sulfide deposits. *Journal of Earth Sciences and Environment*, 29(4): 331–344
- Li Xiaohu, Chu Fengyou, Lei Jijiang, et al. 2008. Advances in slow-ultraslow-spreading Southwest Indian Ridge. *Advances in Earth Science*, 23(6): 595–603
- Liang Ting, Wang Denghong, Qu Wejun, et al. 2007. REE geochemistry of calcites in the Dachang tin-polymetallic deposit, Guangxi. *Acta Petrologica Sinica*, 23(10): 2493–2503
- Liu Yanguang, Meng Xianwei, Fu Yunxia. 2005. Rare earth element and strontium-neodymium isotope characteristics of hydrothermal chimney in Jade area in the Okinawa Trough. *Acta Oceanologica Sinica*, 27(5): 67–72
- Lottermoser B G. 1992. Rare earth elements and hydrothermal ore formation processes. *Ore Geology Reviews*, 7(1): 25–41
- Michard A. 1989. Rare earth element systematics in hydrothermal fluids. *Geochim Cosmochim Acta*, 53: 45–759
- Michard A, Alharedo F. 1986. The REE contents of some hydrothermal fluids. *Chemical Geology*, 53: 31–60
- Michard A, Albaredo F, Michard G, et al. 1983. Rare earth elements and uranium in high-temperature solutions from East Pacific Rise hydrothermal field 13°N . *Nature*, 303: 795–797
- Münch U, Lalou C, Halbach P, et al. 2001. Relict hydrothermal events along the super-slow Southwest Indian spreading ridge near $63^\circ 56' \text{E}$ -mineralogy, chemistry and chronology of sulfide samples. *Chemical Geology*, 177(3–4): 341–349
- Rimstidt J D, Balog A, Webb J. 1998. Distribution of trace elements between carbonate minerals and aqueous solutions. *Geochim Cosmochim Acta*, 62: 1851–1863

- Rona P A, Klinkhammer G, Nelsen T A, et al. 1986. Black smokers, massive sulphides and vent biota at the Mid-Atlantic Ridge. *Nature*, 321: 33–37
- Shuang Yan, Bi Xianwu, Hu Ruizhong, et al. 2006. REE geochemistry of hydrothermal calcite from tin-polymetallic deposit and its indication of source of hydrothermal ore-forming fluid. *Mineral Petrol*, 26(2): 57–65
- Song Xuechun. 2009. Which lasted 300 days, accumulated more than 46,000 sea miles sailing-“Da Yang Yi Hao” full return? *People’s Daily*, 03–18(5)
- Tao Chunhui, Lin Jian, Guo Shiqin, et al. 2007. Discovery of the first active hydrothermal vent field at the ultraslow spreading Southwest Indian Ridge: the Chinese DYI 15–19 Cruise. *Ridge Crest News*, 16: 25–26
- Terakado Y, Masuda A. 1988. The coprecipitation of rare earth elements with calcite and aragonite. *Chem Geol*, 69: 103–110
- Wood S A. 1990. The aqueous geochemistry of the rare-earth elements and yttrium: 1. Review of available low-temperature data for inorganic complexes and the inorganic REE speciation of natural waters. *Chem Geol*, 82: 159–186
- Zeng Zhigang, Zhai Shikui, Zhao Yiyang, et al. 1999. Rare earth element geochemistry of hydrothermal sediment from the TAG hydrothermal field, Mid-Atlantic Ridge. *Marine Geology and Quaternary Geology*, 19(3): 59–66
- Zhong S, Mueei A. 1995. Partitioning of rare earth elements (REEs) between calcite and seawater solutions at 25 °C and 1 atm, and high dissolved REE concentration. *Geochim Cosmochim Acta*, 59: 443–453